Relationship Between the Process of Large-scale Sediment Movement and Ground Vibration

Hiroshi ASAHARA[1*], Atsuhiko KINOSHITA[2], Yasutaka TANAKA[3], Hiroaki SUGAWARA[3], Gengo YOSHIMURA[3], Wataru SAKURAI[2], Teruyoshi TAKAHARA[2] and Soichi KAIHARA[4]

[1] KANAME Technological Development Co., Ltd. (2-7-4 Torigoe, Taito-ku, Tokyo 1110054, Japan)

[2] National Institute for Land and Infrastructure Management, MLIT (1 Asahi, Tsukuba, Ibaraki 3050804, Japan)

[3] Sediment Disaster Prevention Technology Center, Kinki Regional Development Bureau, MLIT (3027-6 Ichinoro, Nachikatsu-ura Town, Higashimuro-gun, Wakayama 6495302, Japan)

[4] Eight-Japan Engineering Consultants Inc. (3-1-21 Tsushimakyoumachi, Kita-ku, Okayama, Okayama 7008617, Japan)

*Corresponding author. E-mail: asahara@kaname-tec.co.jp

Vibration sensors are expected to be used as an effective means of detecting a large-scale sediment movement triggered by rainfall. However, there is as yet no clear understanding of the relationship between ground vibration and the process of large-scale sediment movement. So we analyzed the relationship, comparing ground vibration of high frequency range (higher than 1 Hz) to vibration of low frequency range (lower than 0.1 Hz) for the Akadani large-scale landslide in Japan in 2011, and comparing video images with seismic data for its re-collapse in 2014. We can explain observation facts consistently, assuming that high frequency vibration is generated by the impact when crushed soil collides with the riverbed or the opposite bank, and that low frequency vibration occurs only when the rock mass slides down without being crushed. High frequency vibration can be used for collapse detection, and the direction of the collapse can be easily estimated using low frequency vibration close to the collapse if it is observed, although low frequency vibration is often not observable due to the collapse process. Furthermore, the detailed process of Akadani landslide was verified from the time difference of vibration observed for each frequency band.

Key words: Large-scale landslide, Sediment movement process, Seismic wave, Video image

1. INTRODUCTION

When a large-scale deep-seated landslide occurs and it forms a landslide dam, submergence damage by flooding can occur in the upstream area and large flood damage can be caused by natural dam breakdown in the downstream area. In a large-scale rain disaster in which deep-seated landslide occurs in multiple places, it usually takes much time to find landslide dams due to bad weather or blocking of the transportation network.

It is known that a high sensitivity seismic network with some 20 km interval stations can detect small ground vibration caused by a deep-seated landslide [e.g., *Moriwaki*, 1999; *Ohsumi et al*., 2005, 2006; *Yamada et al*., 2012]. As such, vibration sensors are expected to be used as an effective means of detecting a large-scale sediment movement triggered by rainfall. MLIT (Ministry of Land, Infrastructure, Transport and Tourism), Japan is now developing an automatic deep-seated landslide detection system using real-time seismic data. MLIT has constructed about 200 seismograph observation stations around areas with high deep-seated landslide probability, and uses Hi-net (High sensitivity seismic observation network) data whose network consists of about 800 stations by NIED (National Research Institute for Earth Science and Disaster Resilience). MLIT plans to use this information for providing to local governments and finally leading to provision of disaster information to citizens. However, there is as yet no clear understanding of the relationship between ground vibration and the sediment movement process.

In this study, we compared ground vibration in the range of 1 – 7 Hz and low frequency ground vibration in the range of 0.01 – 0.1 Hz, which were caused by the Akadani large-scale landslide in Gojo City, Nara Prefecture, Japan on September 4, 2011 to establish the sediment movement process and the

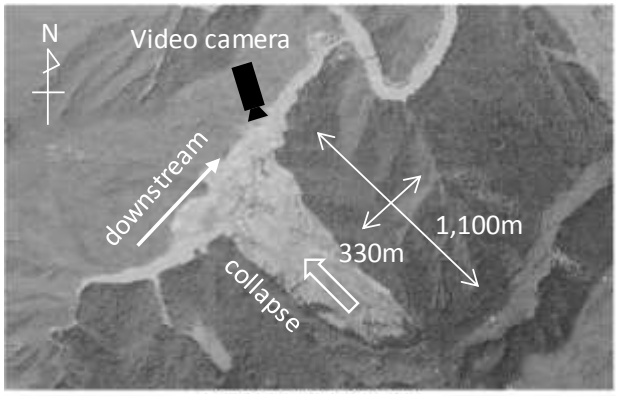

Fig. 1 Top view of the Akadani landslide. It also shows the position and shooting direction of the video camera installed for collapse monitoring (Fig. 7).

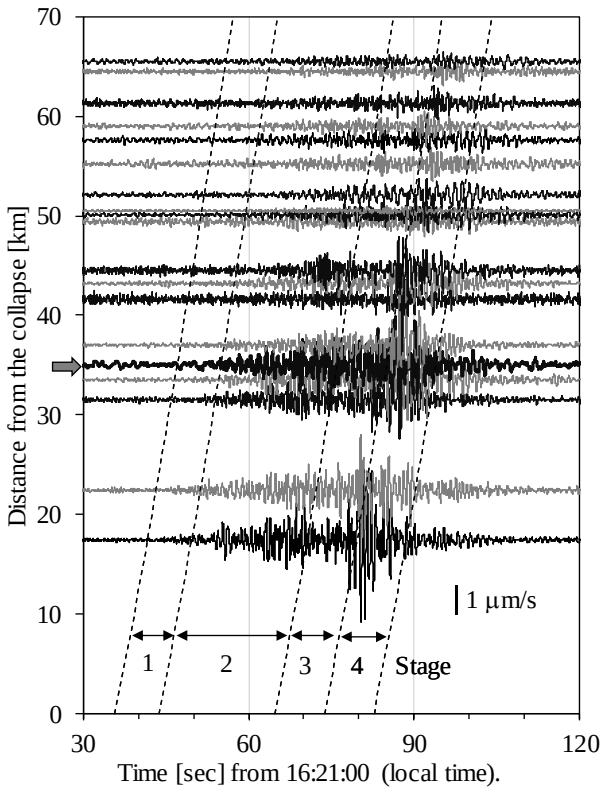

Fig. 2 1 − 7Hz filtered velocity waveforms of vertical component of the Akadani landslide in 2011. The waveforms are arranged by distance from the collapse. Adjacent records are shown alternatingly in black and gray for clarify. The oblique dashed lines correspond to each stage shown in Fig. 3. The arrowed waveform at 35.1 km is F-net Nokami station, whose data is analyzed in Fig. 3 and Fig. 4.

mechanism causing ground vibration. Video images recorded at the re-collapse on August 10, 2014 were also examined comparing with seismic data.

2. GROUND VIBRATION CAUSED BY AKADANI LANDSLIDE IN 2011

On September 3 – 4, 2011, over 30 large-scale sediment movements occurred across a wide region

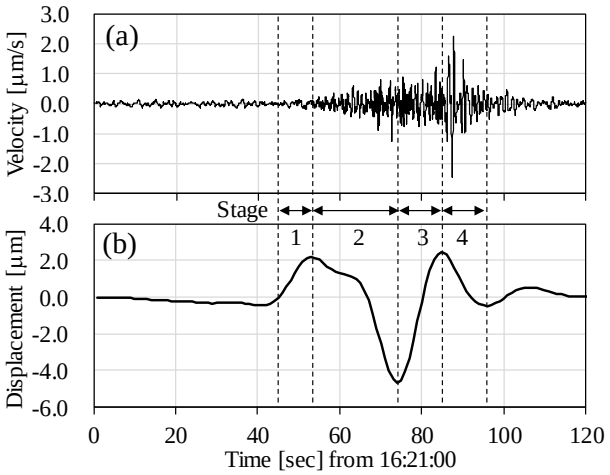

Fig. 3 Vertical components of (a) 1 − 7 Hz velocity and (b) 0.01 − 0.1 Hz displacement waveforms observed at F-net Nokami station.

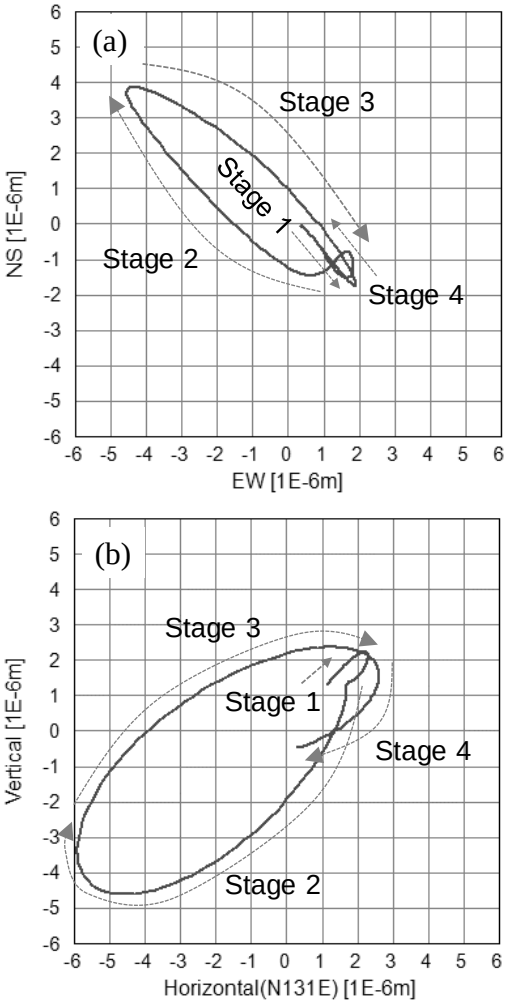

Fig. 4 0.01 − 0.1 Hz particle motion of F-net Nokami station (a) in a horizontal plane and (b) in a vertical plane along slope direction (N131°E).

of the Kii Peninsula, as Typhoon Talas (2011) produced heavy rainfalls across western Japan, and 17 river channels were blocked by landslide dams.

The Akadani landslide, one of the largest events, occurred at 16:21 on September 4, 2011 (local time) in Nara Prefecture, Japan (34.127°N, 135.725°E). **Fig. 1** shows the collapse area. The collapse occurred from a ridge at an altitude of 1,050 m. The area was about 330 m width in average, 1,100 m length along the slope and the collapsed volume was 9.3 million m^3. The direction of collapse was northwest (parallel to the slope; N131°E), and the slope angle was 33°.

Fig. 2 shows seismic records (applying a band-pass filter of 1 – 7 Hz to velocity vertical components) of the Akadani landslide by Hi-net and the broadband seismic network F-net. These seismic networks are both operated by NIED. Here we have studied with the filter of 1 – 7 Hz band, since the dominant frequency of vibration accompanying the deep-seated landslides is analyzed to be about 1 – 3 Hz [*Moriwaki*, 1999; *Ohsumi et al*., 2005, 2016]. The waveforms are arranged by distance from the collapse (This graph is called a record section). Vibration due to the collapse was observed at even 70 km ahead. The oblique dashed lines correspond to each stage shown in **Fig. 3**. The slopes of these lines show that these seismic wave propagations are explained by S wave velocity. The times when the dashed lines cross 0 km represents the moment when each phenomenon occurred at Akadani area. The collapse start time is assumed to be 16:21:35.

Fig. 3 shows the vertical components of 1 – 7 Hz velocity and 0.01 – 0.1 Hz displacement waveforms, observed at F-net Nokami station, 35.1 km away from Akadani area, which is the nearest broadband seismograph station from the collapse. Stages in the figure are explained in **Table 1**. The displacement waveforms were obtained by performing Fourier transformation on the velocity waveform, integrating once in the frequency domain and performing inverse Fourier transformation to the time domain. **Fig. 4** shows the 0.01 – 0.1 Hz particle motions of Nokami station in a horizontal plane and in a vertical plane along the slope from Stage 1 to 4. The orbit which the particle motion draws almost coincided with the slope direction (**Fig. 1**).

In order to explain the sediment movement process using ground vibration data, it was assumed that the dominant frequency of vibration represents the size of rocks which generate vibrations. We assumed that larger rock masses may produce vibration of lower frequencies. In particular, (1) the low frequency (0.01 – 0.1 Hz) displacement waveform corresponds to a large force exerted on the ground in one direction when a large rock mass collides against the opposite bank without being crushed, and (2) the high frequency (1 – 7 Hz) velocity waveform represents the collision of fractured sediments against the riverbed or the opposite bank.

Table 1 shows the relationship between low

Table 1 Relationship between low frequency or 1 – 7 Hz vibration data and sediment movement.

Stage	Horizontal displacement	Vertical displacement	Time duration	1 – 7 Hz velocity	Interpretation of sediment movement
1	Towards↘ southeast	Upward	8 sec.	No vibration	Start of movement of the rock mass and reaching the riverbed
2	Towards↖ northwest	Downward	21 sec.	Start of vibration	Collision of the rock mass with the opposite bank
3	Towards↘ southeast	Upward	9 sec.	In the midst of increasing	Reaction to displacement (continued flowing down of fractured sediment)
4	Slight change	Downward	9 sec.	Peak	Settlement (flowing down of fractured sediment)

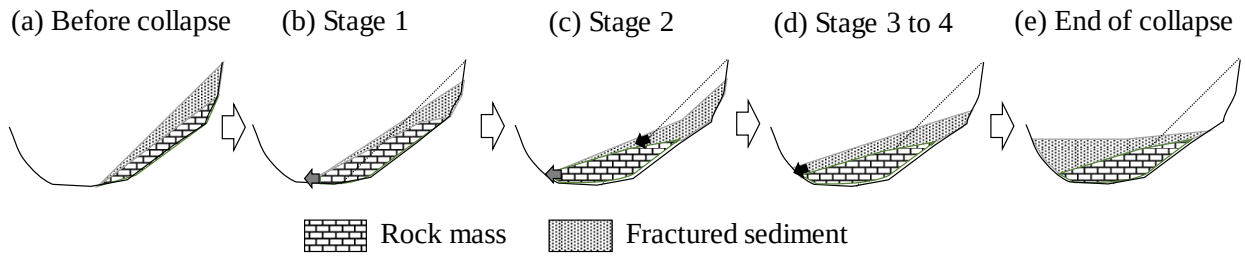

Fig. 5 Sedmient movement process estimated from ground vibration data. (a) Before collapse: fractured soil is accumulated on the rock mass. (b) Stage 1: Start of movement of the rock mass. The rock mass has not reached the opposite bank yet. (c) Stage2: Collision of the rock mass with the opposite bank. The fractured sediment flows on the rock mass. (d) Stage 3 to 4: The fractured sediment continued flowing down after the settlement of the sliding rock mass. (e) End of collapse.

frequency and high frequency vibration data at each stage, and **Fig. 5** shows our sediment movement process model of this landslide considering the above two hypotheses. Before collapse, fractured sediment is accumulated on the rock mass. In Stage 1, the rock mass starts to move but has not reached the opposite bank yet. The fractured sediment still moves almost together with the rock mass. At this period, the upward force is inferred to be caused by the friction force of the descending rock mass and no vibration was observed for high frequency. In the following Stage 2, the rock mass collides with the opposite bank, so the force changed to the downward. The high frequency vibration starts increasing, as the fractured sediment starts to flow down on the rock mass, then collides with the riverbed and the opposite bank. As there was no factor causing upward force after the collision in Stage 2, Stage 3 and 4 are inferred to be a reaction to the former stage. Particle motion of low frequency almost moves on the slope surface through 4 stages. On the contrary, the high frequency vibration increases around Stage 3, and peaked in Stage 4. The fractured sediment is still flowing down even after the settlement of the sliding rock mass, so the high frequency vibration is in the midst of increasing and peak time for high frequency delayed by some ten seconds. The inferred sediment movement process is the collision of transported rocks with the riverbed and the opposite bank at first, followed by the deposition of fractured sediment. The relationship between high frequency vibration and the movement of fractured sediment was confirmed by video image in Chapter 3 later.

This model can explain the following two observed facts without contradiction.

Fact 1: The geological structure of the landslide dam in Akadani area shows a little fractured sliding rock mass layer at the bottom and fractured collapsed sediment above this layer [*Sakurai et al*., 2015].

Fact 2: The low frequency vibration is observed several ten seconds earlier than high frequency vibration.

3. GROUND VIBRATION CAUSED BY AKADANI LANDSLIDE IN 2014 AND VIDEO IMAGES

A re-collapse occurred at Akadani area at 07:27 on August 10, 2014 by Typhoon Fengshen (2014). The collapsed volume was estimated to be 0.76 million m^3. This collapse was filmed in a video camera by MLIT for collapse monitoring. The position and shooting direction of the video camera is shown in **Fig. 1**. MLIT had also started to operate seismic stations about 9.5 km away from Akadani area and succeeded in measuring the vibration of this event. **Fig. 6** shows seismic records (applying a band pass filter of 1 – 7 Hz to velocity vertical components) by Hi-net, F-net and MLIT seismic observation network. The waveforms are arranged by distance from the collapse. **Fig. 7** is video images at the moment (a) when the collapsed front reached the riverbed, (b) when the collapsed front collided against the opposite bank and (c) when the collapsed front was presumed to reach the highest altitude of the opposite bank, splash by the collision reached the highest. The oblique dashed lines in **Fig. 6** show propagation of S waves departing at the video image times of **Fig. 7**.

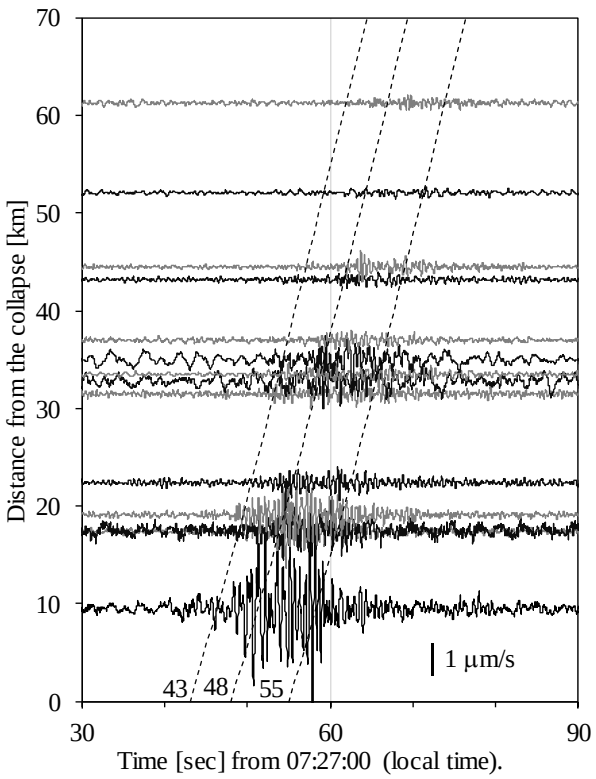

Fig. 6 1 – 7Hz filtered velocity waveforms of vertical component of the Akadani re-collapse in 2014. The waveforms are arranged by distance from the collapse. Adjacent records are shown alternatingly in black and gray for clarify. The oblique dashed lines correspond to the video image times in Fig. 7.

We compared the video images and vibration data at 9.5 km away from the collapse, considering the travelling time of seismic wave. Almost no ground vibration was observed during collapsed sediment flowing down the slope (prior to 07:27:43). Although it was difficult to identify the start time of collapse since the video images were unclear due to raindrops and dust, it was confirmed

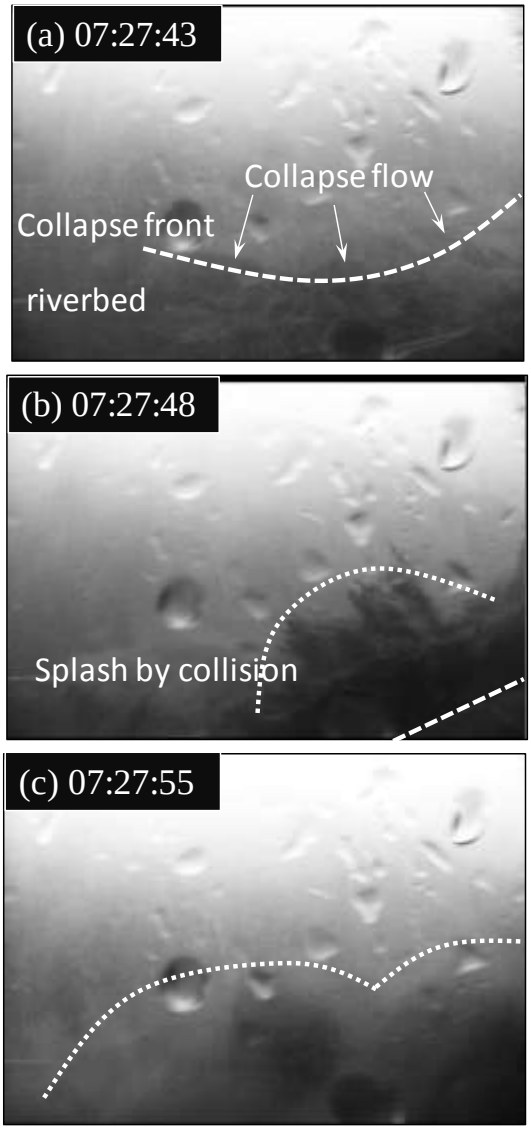

Fig. 7 Video images at the secondary collapse in 2014 from the opposite bank. White dashed lines show the collapse front of fractured sediments and dotted lines show the splash of soils accompanying with the collision with the opposite bank.
(a) 07:27:43; The collapsed front reached the riverbed. (b) 07:27:48; The collapsed front collided against the opposite bank. (c) 07:27:55; The collapsed front was presumed to reach the highest altitude of the opposite bank.

that the sediment was flowing down the slope at 07:27:35 at the latest even from the unclear video images. It was found that high frequency vibrations were hardly observed when the soils were flowing down the slope.

The vibration started when the collapsed sediment reached the riverbed (07:27:43), and the amplitude reached the first peak at the moment when the fractured sediment collided with the opposite bank (07:27:48). The second peak 07:27:55 is the moment when the collapsed front reached the highest altitude of the opposite slope. It is thought that the soils reached the maximum elevation was not the cause of the vibration peak, but that the collision of soils flowing down from the subsequent high elevation to the riverbed or the opposite bank was the cause. After the collapse front reached the highest altitude of the opposite slope (07:27:55), the vibration settled down. The collapsed soil is inferred to be a state where crushing has advanced since the sediment flowing down seems to have high fluidity from the video images. These results make it clear that the collision of fractured sediment to the riverbed and to the opposite bank causes the 1 – 7 Hz vibration.

Although 1 – 7 Hz vibration was observed, 0.01 – 0.1 Hz vibration was not observed at any broadband seismic stations including at the MLIT observation station closest to 9.5 km to the collapse (Broadband seismographs are used for MLIT stations).

4. DISCUSSION

4.1 Relationship between the landslide process and ground vibration

The relationship between ground vibration and sediment transport process can be arranged as follows from the low frequency and high frequency vibration data of 2011 Akadani landslide and the vibration data and video images of 2014 re-collapse.

High frequency vibration is generated by the impact when crushed soil collides with the riverbed or the opposite bank. Therefore, the small-scale landslide detection by vibration sensors is difficult as large ground vibration does not occur in a small-scale collapse such that the soils stop on the slope sliding. On the other hand, in a collapse that causes river blockage, large amount of soil collides against the riverbed and the opposite bank, so there is a high possibility that it can be detected with vibration sensors.

Low frequency vibration occurs only when the rock mass slides without being crushed, conversely it does not occur when it falls apart at the moment of landslide occurrence.

From the time difference between low frequency vibration and high frequency vibration, it is considered that the rock mass first slide without being crushed, then the upper fractured sediment flowed down.

4.2 Low frequency vibration

Fig. 8 shows deep-seated landslide cases whether low frequency vibration was observable or not for each distance from the collapse. In general, the larger the size of the collapses are, the more cases are observable. However, there are some cases

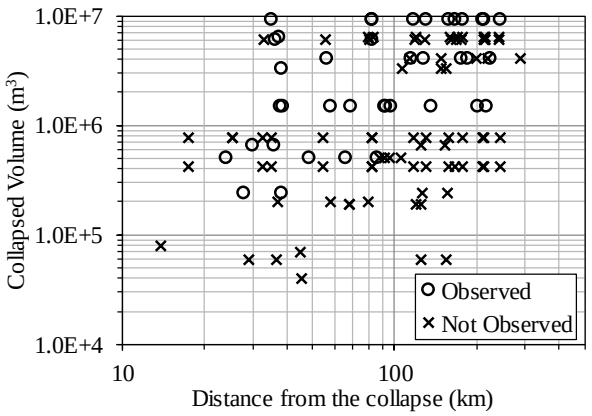

Fig. 8 Deep-seated landslide cases whether low frequency vibration was observable or not for each distance from the collapse.

that low frequency vibrations are not observed for exceeding 5 million m^3 volume, despite in other cases low frequency vibrations are observed for smaller than 1 million m^3. Considering that low frequency vibration occurs only when the rock mass slides without being crushed, whether it is observable or not is influenced by the process of collapse. The low frequency vibration was also observable at the stations 200 km away in 2011 Akadani landslide, but it was not observed at the station nearest 9.5 km in the re-collapse of 2014. The re-collapse is considered that low frequency vibration did not occur because the sediment flowing down has high fluidity, judging from the camera images in addition to being small volume. Large scale landslides are always observable by high frequency vibration, but low frequency vibration is not necessarily observed even if the scale is large. Therefore, it is more effective to use high frequency vibration than low frequency vibration to detect the occurrence of collapse. Moreover, the earthquake including the teleseismic earthquake influence greatly in the low frequency band. In the case of Magnitude 6 class or larger teleseismic earthquake, a few minutes of vibration is observed in the high frequency band, whereas in the low frequency band it may last for more than two hours. This also makes it difficult to use the low frequency band for landslide detection.

Inversion analysis is generally required to obtain the force acting on the surface (source time function) from the low frequency waveforms observed at multiple points [*Kanamori and Given*, 1982; *Yamada et al*., 2013]. However, a displacement waveform obtained at the point where is sufficiently nearer than one wavelength from the collapse shows almost the same shape as the force acting on the surface, as the influence of reflection or scattering due to underground discontinuities and inhomogeneities is small. This property is useful from the viewpoint of engineering. Assuming that S wave velocity is 3 km/s, the wavelength of 50 seconds period vibration is 150 km. When the observation point is far from the collapse, the particle motion deviates from the collapse direction and draws a complicated shape. **Fig. 4** shows that we can know the direction of the collapse from particle motion even at 35 km away from the collapse. Therefore, it was found that the force acting on the surface can be roughly and easily known from the displacement waveform even at the distance of about 1/4 wavelength which is sufficiently shorter than one wavelength, without complicated inversion analysis. Although low frequency vibration is not necessarily observed, if the vibration is observed at a nearby point and the position estimation by high frequency vibration is accurate, there is a possibility that it can be used for judging the presence or absence of river channel blockage.

5. CONCLUSION

The relationship between the deep-seated landslide process and the ground vibration was analyzed from the vibration data of two frequency bands and video images. As a result, it is not contradictory to the observation facts, assuming that high frequency (higher than 1 Hz) vibration is generated by the impact when crushed soil collides with the riverbed or the opposite bank, and that low frequency (lower than 0.1 Hz) vibration occurs only when the rock mass slides without being crushed. High frequency vibration can be used for the detection of collapse compared more effectively than low frequency band, because high frequency vibration is observed at any time as the scale of collapse is large, and less affected by teleseismic earthquakes than low frequency band. Furthermore, if the low frequency vibration is observed at the station within about 35 km from the collapse site, the direction of the collapse can be easily estimated by particle motion, but low frequency vibration is often not observable due to the collapse process. If the low frequency vibration is observed at a nearby point and the position estimation by high frequency vibration is accurate, there is a possibility that it can be used for judging the presence or absence of river channel blockage.

In this study, we examined the landslide process for Akadani area. However, different interpretations might be possible for the collapse that occurs under different conditions. It is necessary to conduct the

same examination for other cases for verifying the validity of interpretation of this study.

ACKNOWLEDGMENT: We acknowledge the National Research Institute for Earth Science and Disaster Resilience (NIED) for the use of the seismic data (Hi-net and F-net).

REFERENCES

Kanamori, H. and Given, J. (1982): Analysis of long-period seismic waves excited by the May 18, 1980, eruption of Mount St. Helens – a terrestrial monopole, Journal of Geophysical Research, Vol. 87, No. B7, pp. 5422 – 5432.

Moriwaki, H. (1999): Characteristics of a ground seismogram due to a debris flow originating from a landslide -a Gamaharasawa debris flow-, Journal of Japan Landslide Society, Vol. 36, No. 3, pp. 99 – 107 (in Japanese with English abstract).

Ohsumi, T., Asahara, H. and Shimokawa, E. (2005): Analysis of ground-vibration induced by the 10 August 2004 Ohtou landslide in Nara Prefecture, Japan using the data of high sensitivity seismograph network: Application to landslide detecting, Journal of Natural Disaster Science, Vol. 24, No. 3, pp. 267 – 277 (in Japanese with English abstract).

Ohsumi, T., Asahara, H. and Shimokawa, E. (2006): Hypocenter detecting analysis using the data of high sensitivity seismograph network applied for the mass movement on Mt. Shirouma, Nagano in 2005, Journal of the Japan Landslide Society, Vol. 43, No. 1, pp. 27 – 32 (in Japanese with English abstract).

Ohsumi, T., Kaihara, S., Sakai, R. and Sakurai, W. (2016): Verifications of the noise reduction by down hole sentinel vibration sensors for “Deep-seated landslide detection” and “Detectable landslide volume” in the Kii peninsula, Journal of the Japan Society of Erosion Control Engineering, Vol. 68, No. 5, pp. 32 – 37 (in Japanese with English abstract).

Sakurai, W., Sakai, R., Okuyama, Y., Ogawauchi, Y., Fukuda, M., Sato, M., Kaihara, S., Tadakuma, N. and Fujiwara, Y. (2015): Differences in hydrological and erosion conditions caused by the internal structure of a landslide dam, Journal of the Japan Society of Erosion Control Engineering, Vol. 68, No. 3, pp. 21 – 30 (in Japanese with English abstract).

Yamada, M., Matsushi, Y., Chigira, M. and Mori, J. (2012): Seismic recordings of landslides caused by Typhoon Talas (2001), Japan, Geophysical Research Letters, Vol. 39, L13301, doi:10.1029/2012GL052174.

Yamada, M., Kumagai, H., Matsushi, Y. and Matsuzawa, T. (2013): Dynamic landslide process revealed by broadband seismic records, Geophysical Research Letters, Vol. 40, No. 12, pp. 2998 – 3002.